21, rue d'Artois, F-75008 PARIS
http : //www.cigre.org

CIGRE US National Committee
2021 Grid of the Future Symposium

Comparative Study of the Reactive Power Consumption of a Dominion Energy Virginia Autotransformer due to Geomagnetically-induced Current

A.A. ADEMOLA, X. LI, D. YANG, M.J. TILL, Y. LIU
Dominion Energy Virginia
USA

SUMMARY

Geomagnetically-induced currents (GIC), primarily caused by extreme space weather, are abnormal quasi-DC currents that can flow into the power system with serious implications for the reliability and safety of the grid. One of the principal effects of GIC is a significant increase in reactive power consumption of grounded wye-connected transformers which serve as junctions for GIC to flow into and out of the power grid. To foster understanding of this phenomenon, this paper compares the relationship between GIC and reactive power consumption of an autotransformer at a Dominion Energy substation in Virginia for real operating conditions and realistic system topologies. The findings show that GIC-induced reactive power consumption is largely independent of system conditions; however, it has a significant transient buildup period, up to several minutes, which can lead to overestimation of its magnitude for short-duration GIC.

KEYWORDS

Autotransformer, Geomagnetic Disturbance, Geomagnetically-Induced Currents, Reactive Power Consumption.

aademol1@vols.utk.edu

1 Introduction

Geomagnetically-induced currents (GIC) are quasi-DC currents that flow between the earth and the electric grid due to cyclical solar activities interacting with the earth's magnetosphere. These interactions disturb the Earth's geomagnetic field, often called a geomagnetic disturbance (GMD), which in turn causes a geoelectric field to be induced in the conductive earth's surface. The electric power grid, usually grounded at wye-connected transformer neutrals, becomes susceptible to the inflow and outflow of GIC during occurrences of this phenomenon. When such quasi-DC current flows through the transformers, it can cause transformer half-cycle saturation which leads to large increase in reactive power consumption, the generation of hotspots on winding and structural components, and the production of even and odd harmonics. On a system-wide level, the large increase in reactive power consumption can lead to voltage collapse and blackouts, while the injection of even harmonics, which the power system is generally not hardened against, can cause misoperation of protection systems, trip off static VAR compensators (SVC), and overheat generators [1], [2].

The most often-used illustration of the devastating effect of GIC is the Hydro Quebec blackout in 1989 which took 21,500 MW of generation offline, plunged 9 million people into darkness, and caused major social and economic losses [3], [4]. Other notable GIC events include the tripping of thirteen 115 kV capacitor banks in the Dominion Energy Virginia (DEV) transmission network during the same 1989 event [5], tripping of SVCs and transformer damage in New Zealand in 2001 [6], and power blackouts experienced by 50,000 people in southern Sweden in 2003 [7], among others.

Studies have shown that the maximum amplitude of GMD-induced geoelectric fields is about 10 times higher at locations above $50^0 - 55^0$ latitude threshold, and about 5 times larger on poor conductivity ground than good conductivity ground [8, 9]. Even though DEV's system is located below the latitude threshold, it is situated on a poor ground conductivity region; thus the DEV grid is still susceptible to some GMD impacts. For this reason, and to comply with NERC's reliability standard on GMD operations (EOP-010-1 [10]), DEV has made several efforts to model and study geoelectric scenarios, harden equipment against GIC, and improve system operators' situational awareness [5]. To further these efforts, this study investigates the relationship among GIC magnitudes, transformer saturation time, and reactive power consumption for different transformer load levels and under different system contingencies.

It is well known that the additional reactive power consumption of a transformer due to GIC, Q_{GIC}, can be estimated using Equation 1.

$$Q_{GIC} = Q - Q_0 = K \cdot I_{eff} \tag{1}$$

Q is the total reactive power consumption, Q_0 is the reactive power consumption during normal operation without GIC, and I_{eff} is the effective GIC flowing in the transformer windings, which depends on the transformer type [11]. For an autotransformer, I_{eff} is calculated as shown in Equation 2.

$$I_{eff} = \frac{(N-1)I_s + I_c}{N} \tag{2}$$

$$N = \frac{N_s + N_c}{N_c} \tag{3}$$

Where I_c, I_s, N_c, and N_s, are the currents and number of turns in the autotransformer common and series windings respectively.

K in Equation 1 is a constant that determines the relationship between Q_{GIC} and I_{eff}. Accurate determination of K values usually requires measurement tests during transformer pre-commissioning [12]. Previous studies have either used generic K values based on transformer core design [13], or simulated DC injection tests to estimate its value for a particular transformer [12]. However, these works did not consider the possible changes in K values under different grid operating conditions as posited in [14]. Furthermore, previous works have either focused on reactive power consumption after saturation is complete [12], or time required for the transformer to saturate under GIC or DC excitation [15]. This

study considers both, in order to provide a more holistic reference for system operators who wish to understand both the transient and steady-state GIC impacts on their network equipment.

The rest of the paper is organized as follows. Section 2 of this paper highlights the modeling of a DEV substation and model validation. Section 3 considers operating conditions and the simulation setup to investigate the relationship between GIC, reactive power consumption, and saturation time. Section 4 reports the simulation results, while remarks and conclusions are presented in Section 5.

2 MODELING OF THE DEV SUBSTATION AND TRANSFORMERS

An ASPEN OneLiner model of DEV's transmission network was used to create a Thevenin equivalent model, which represents the whole network from the point of view of two substation buses as shown in Figure 1. The modeled substation has a GIC monitor at the neutral of one of its transformers and GIC with maximum peak of 6 A has been measured as recently as March 2021. This substation has two 504 MVA grounded wye-connected autotransformers, T1 and T2, connecting the 500 kV Bus 1 to the 230 kV Bus 2. The third wye-wye connected transformer, T3, is a virtual transformer that represents the network connections between the two buses that are external to the substation. The voltage sources G1 and G2 are also virtual, and they represent the equivalent boundary conditions of the network at each bus.

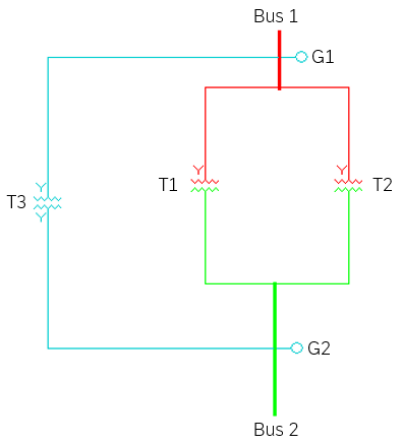

Figure 1: Thevenin equivalent of the DEV substation

The network data are presented in Table 2. Note that the positive sequence impedance equals the synchronous, transient, and sub-transient impedances. These data were used to build an analogous transient model in PSCAD/EMTDC, since electromagnetic transient tools are expected to be more accurate for GIC impact analysis than load flow-based tools [16]. To accurately model the zero-sequence impedance of T3, which is larger than its positive sequence impedance, a compensating impedance was added to the neutral of T3 to account for the difference [17].

Table 1: Network Data

Network Equipment	**Operating voltage (kV)**	**Voltage level (pu)**	**Rating (MVA)**	**Positive Sequence Impedance (pu based on 100 MVA)**	**Zero Sequence Impedance (pu based on 100 MVA)**
Bus 1	500				
Bus 2	230				
G1	500	$1.03\angle 30.2^0$	100	0.00021 + j0.0063	0.0013 + j0.012
G2	230	$0.98\angle 30.6^0$	100	0.00245 + j0.02	0.0059 + j0.02
T1 & T2	500/230		500	0.00017 + j0.016	0.00017 + j0.016
T3	500/230		0	0.0028 + j0.0053	0.0053 + j0.052

A simple fault study was used to validate the correctness of the transient model in comparison to the original network model as presented in Table 3. For all fault simulations, the absolute error of the transient model is less than 1%, thereby proving that it is a reliable duplicate of the original model.

Table 2: Fault study to validate transient model

Fault Location	Fault Type	Original model fault current (kA)	Transient model fault current (kA)	% Absolute Error
Bus 1	3φ-to-ground	23.06∠-57.1	23.12∠-57.7	0.26%
	Line-to-Line	11.45∠-57.1	11.56∠-57.7	0.96%
Bus 2	3φ-to-ground	32.64∠-56.0	32.42∠-56.6	0.67%
	Line-to-Line	16.26∠-55.9	16.32∠-56.6	0.37%

To model the saturation characteristics of autotransformers T1 and T2, parameters including air core reactance, knee voltage, and magnetizing current were utilized. A well-known rule-of-thumb was used to estimate the air-core reactance to be twice the transformer leakage reactance [17]. The knee voltage, $V_{knee,}$ and magnetizing current, I_m, were estimated by inputting the measured transformers' V-I data points into a curve-fitting optimization module specifically designed for this purpose in PSCAD/EMTDC [18]. Figure 2 shows the transformers' saturation curve and the approximate curve corresponding to the derived V_{knee} and I_m, and indicates that the derived parameters are accurate enough to model the saturation characteristics of the transformers.

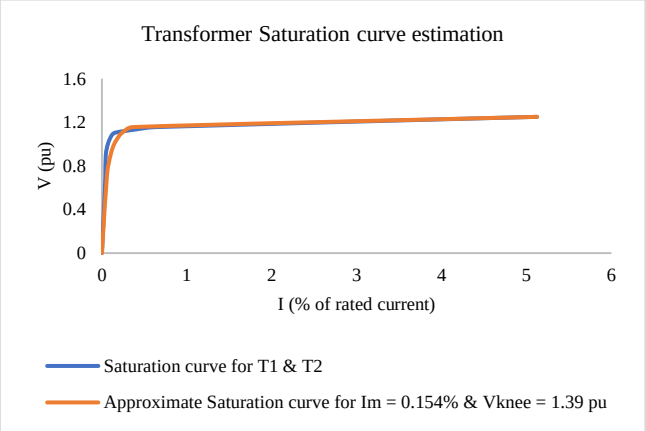

Figure 2: Comparison of measured saturation curve and approximate saturation curve corresponding to Im & Vknee

3 DC INJECTION TEST AND INVESTIGATED OPERATION CONDITIONS

A DC injection test was implemented to simulate the flow of the GIC from the ground to the neutral of T1. This involved the use of a PI controller with a proportional gain of 3 and an integral time constant of 0.1s to control the output current, I_{GIC}, of a DC voltage source connected to the neutral of T1. The error signal that controlled the operation of the PI controller was the difference between I_{GIC} and the desired GIC level. It is worth mentioning that I_{GIC} in this work represents the GIC in the transformer neutral, rather than I_{eff} in Equation 2. Neutral GIC is the quantity measured by GIC monitors, and thus is easily obtainable. On the other hand, calculation of I_{eff} requires knowledge of DC distribution in the transformer windings, which depends on relative geographical orientation between the induced geoelectric field and the lines connected to the autotransformer [12]. This may be difficult to accurately compute if the geoelectric field magnitude and orientation are not constant. Since neutral GIC is usually a fraction of I_{eff} [12], this proportionality is subsumed in the relationship between the neutral GIC and reactive power consumption that is considered in this study.

Having set up the transient model for DC injection simulations, the system operating conditions were varied in two ways. First, simulations were ran for different magnitudes of I_{GIC} at the three transformer loading scenarios shown in Table 4. These scenarios represent real operating conditions of the transformers at the selected DEV substation. For instance, the light and heavy load scenarios are the real 2020 spring light and summer peak transformer loads, respectively. Note that the addition of a PQ load was required at Bus 2 to realize the desired loading levels on the transformers. All values correspond to measurements at transformer secondary side.

Table 3: Investigated load scenarios for GIC injection simulations

Investigated Load Scenarios	**Transformer apparent load (MVA)**	**Transformer active load (MW)**	**Transformer reactive load (Mvar)**
Light load	38.4	30.36	23.50
Moderate load	142.6	133.50	50.05
Heavy load	366.3	366.00	13.82

The second set of simulations were carried out in the same way, but for different network topologies in the nearby circuit external to the substation. Network topologies used include the worst-case N-1 and N-2 contingencies that provide the least fault currents at Bus 1, along with the N-0 topology. As expected, the voltage levels and network impedances changed to reflect each change in topology. This required the transient model to be updated accordingly to reflect each topology change. Moreover, the previously described fault simulations were performed for each topology change to validate their corresponding transient models. Table 5 presents the network data for each contingency topology.

For each set of simulations, Q at T1 was recorded to investigate how different operating conditions may influence the relationship between Q_{GIC} and I_{GIC}. Q was simply calculated as the difference between reactive power flow at the primary transformer side and the secondary side.

Table 4: Network data for N-1, and N-2 topology changes

Topology change	**Network Equipment**	**Voltage level (pu)**	**Positive Sequence Impedance (pu based on 100 MVA)**	**Zero Sequence Impedance (pu based on 100 MVA)**
N-1	G1	$1.034\angle 30.0^0$	0.00033 + j0.0098	0.0025 + j0.020
	G2	$0.98\angle 30.57^0$	0.0024 + j0.0198	0.0055 + j0.0198
	T3		0.00277 + j0.029	0.0072 + j0.0565
N-2	G1	$1.036\angle 30.06^0$	0.00039 + j0.0105	0.00245 + j0.0205
	G2	$0.980\angle 30.60^0$	0.0025 + j0.0202	0.0055 + j0.0198
	T3		0.00267 + j0.0282	0.00715 + j0.0567

4 RESULTS AND DISCUSSION

Relationship between Q_{GIC} and I_{GIC} for different load scenarios

To use Equation 1 to compute Q_{GIC}, it is necessary to find the value of Q_0. Hence, the simulation was run for 5 seconds with I_{GIC} = 0 A for each loading scenario. As expected, Q_0 increases as higher current flows through the transformer to serve the increasing load levels as shown in Figure 3. For subsequent simulations, these values of Q_0 were subtracted from Q to obtain Q_{GIC} for corresponding load scenarios.

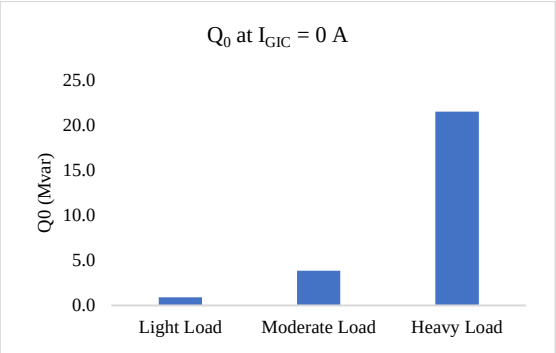

Figure 3: Reactive power consumption at I_{GIC} = 0A

Initially, the DC injection simulations were run for 60 seconds for each loading scenario. Figure 4 shows that the relationship between the Q_{GIC} and the I_{GIC} is not linear as expected from Equation 1. This was found to be due to insufficient simulation time, since Q did not reach a steady state during the simulation time. Therefore, to capture the full extent of change in Q due to GIC injection, much longer simulation times were required as shown in Figure 5.

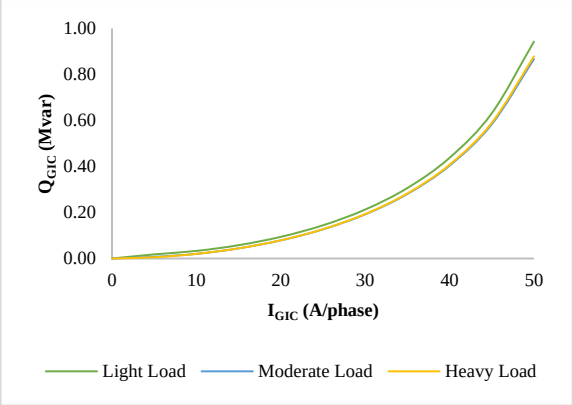

Figure 4: Variation of Q_{GIC} with I_{GIC} for different load scenarios after 60 seconds of simulation

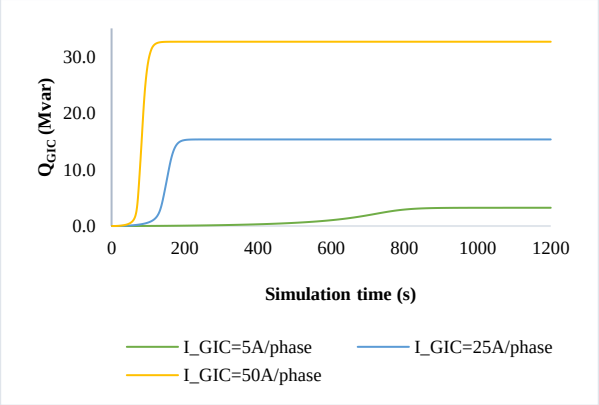

Figure 5: Buildup of Q_{GIC} during simulation for heavy load scenario (Note that injection of I_{GIC} commenced at 10 s)

This slow Q build-up is because the transformer does not saturate immediately after I_{GIC} is injected in its neutral. In fact, saturation is not directly caused by the injection of I_{GIC}, rather, it is a function of the integral of DC voltage applied at the terminals of the transformer's magnetizing circuit [15]. Thus, it is not unusual to run transformer DC excitation tests for up to several minutes to reach steady-state conditions [12], [19]. The simulation times shown in Figure 5 were therefore varied for different ranges of I_{GIC} as follows: 5 – 10A/phase: 1200s, 15 – 30 A/phase: 600s, and 35 – 50 A/phase: 300s. Figure 6 shows the expected linear relationship between the final, steady-state $Q_{GIC,ss}$ and injected I_{GIC} for all load scenarios.

The average slope, K, for all load scenarios varies between 0.64 and 0.66 Mvar/A/phase. This narrow range shows that transformer loading has little effect on the magnitude of $Q_{GIC,ss}$. Therefore, the value of K measured at one load level can be used to estimate the transformer reactive power consumption for other load levels with reasonable accuracy since Q_0 is easily computed. It is worth emphasizing, however, that K is only useful to calculate $Q_{GIC,ss}$. Hence, Equation 1 will not be accurate for the transient regime shown in Figure 5 when Q_{GIC} is still changing.

Given that GIC is not necessarily steady in nature, computation of the time-varying Q_{GIC} before reaching $Q_{GIC,ss}$, say $Q_{GIC}(t)$, will be useful to accurately determine reactive power loss during short GMD events. For example, Figure 5 shows that GIC magnitude of 25 A/phase that occurs for 200 seconds will cause larger reactive power consumption than one with magnitude of 50 A/phase that occurs for 60 seconds.

Therefore, to characterize the time-varying nature of Q_{GIC}, a time constant, T_{GIC}, was defined as the time required for Q_{GIC} to go from its initial value to 63.2% of its final value after GIC injection. The plot of T_{GIC} against I_{GIC} in Figure 7 shows that Q_{GIC} changes faster at larger magnitudes of I_{GIC} and that T_{GIC} is also independent of transformer load levels. However, T_{GIC} has a non-linear relationship with I_{GIC}, thereby complicating the possibility of establishing a generalized mathematical equation to estimate transient $Q_{GIC}(t)$ as a function of K, I_{GIC}, T_{GIC}, and t. Consequently, real-time computation of transient $Q_{GIC}(t)$ may require some non-linear statistical regression modeling. This is a potential direction for future work in this field.

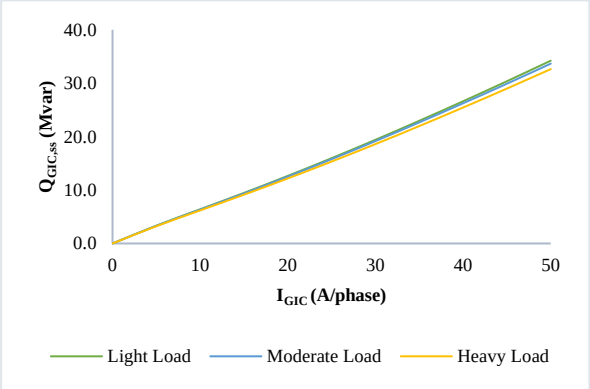

Figure 6: Variation of steady-state $Q_{GIC,ss}$ with I_{GIC} for different transformer load scenarios

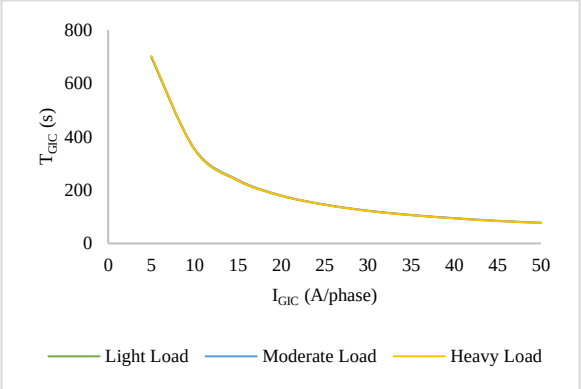

Figure 7: Variation of T_{GIC} with I_{GIC} for different transformer load scenarios

Relationship between Q_{GIC} and I_{GIC} for different system topologies

The relationships between $Q_{GIC,ss}$ and I_{GIC} for the three network topologies during light and heavy loading are presented in Figure 8. It can be observed that the variation in $Q_{GIC,ss}$ at TI due to topology changes is quite small especially at low I_{GIC} magnitudes for both light and heavy loading conditions. Again, this must not be confused with total reactive power consumption, Q, which may still vary significantly since Q_0 can be affected by a change in topology.

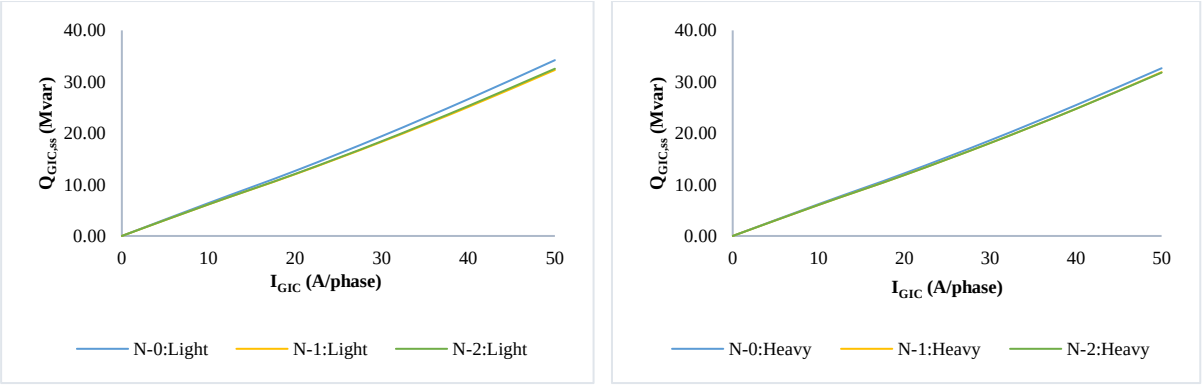

Figure 8: Relationship between $Q_{GIC,ss}$ and I_{GIC} for N-0, N-1, and N-2 system topologies

The results above show that the establishment of K to define the relationship between $Q_{GIC,ss}$ and I_{GIC} at normal operating conditions can still be reasonably accurate after a contingency event changes the network topology. This is a useful result to show that simulation of all possible system conditions is not required to establish a relationship between $Q_{GIC,ss}$ and I_{GIC} at a transformer. Moreover, Fig. 9 shows that T_{GIC} is likewise not significantly affected by network topology changes.

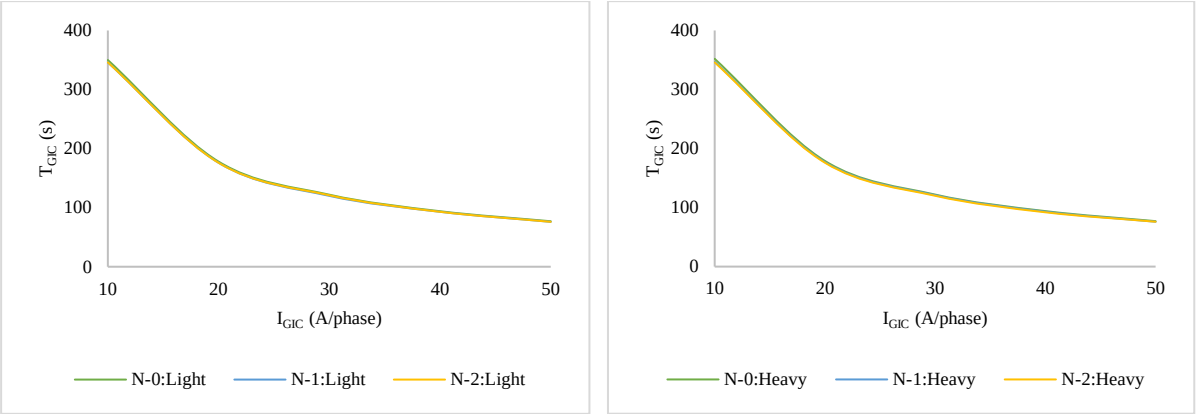

Figure 9: Relationship between T_{GIC} and I_{GIC} for N-0, N-1, and N-2 system topologies

5 CONCLUSION

In this work, a comparative study was performed to investigate the relationship between reactive power consumption, Q_{GIC}, and GIC flowing into the neutral of an autotransformer at a DEV substation. It was shown that there is a linear relationship between these two parameters only after Q_{GIC} reaches steady-state when the transformer is fully saturated. This linear relationship is neither significantly affected by the transformer's loading conditions nor by changes in the topology of the external network. Thus, for a particular transformer, computed value of K at one operating condition and topology can be re-used with reasonable accuracy for other operating conditions and topologies. This reduces the burden of capturing all possible operating conditions and network topologies in the establishment of GIC-to-Q_{GIC} relationship.

A time constant, T_{GIC}, was defined in an attempt to characterize the transient buildup of Q_{GIC} for the autotransformer under the influence of GIC. T_{GIC} was shown to be independent of transformer loading and network topology but dependent on GIC magnitude. This study also revealed that it takes significant time, up to several minutes, for Q_{GIC} to reach steay-state especially for low GIC magnitudes. Thus, consideration of the time-varying $Q_{GIC}(t)$ is necessary for accurate evaluation of the potential effects of short duration GIC. It was also shown that the relationship between T_{GIC} and GIC magntidues is not linear, therefore, the establishment of an easy-to-compute generalized mathematical relationship for $Q_{GIC}(t)$ as a function of GIC, K, T_{GIC}, and time, is complicated. However, this complication presents a direction for future research to use modern non-linear regression tools, such as machine learning algorithm, for real-time computation of $Q_{GIC}(t)$. Simulation data such as the ones generated in this work will be useful to train and test such machine learning algorithms.

BIBLIOGRAPHY

[1] M. Nazir, J. H. Enslin, and M. Babakmehr, "Power System Protection response under Geomagnetically Induced Currents," in *2020 Clemson University Power Systems Conference (PSC)*, 2020-03-01 2020: IEEE, doi: 10.1109/psc50246.2020.9131172.

[2] C. J. Rodger *et al.*, "Geomagnetically Induced Currents and Harmonic Distortion: Storm-Time Observations From New Zealand," *Space Weather*, vol. 18, no. 3, 2020-03-01 2020, doi: 10.1029/2019sw002387.

[3] S. Guillon, P. Toner, L. Gibson, and D. Boteler, "A Colorful Blackout: The Havoc Caused by Auroral Electrojet Generated Magnetic Field Variations in 1989," *IEEE Power and Energy Magazine*, vol. 14, no. 6, pp. 59-71, 2016-11-01 2016, doi: 10.1109/mpe.2016.2591760.

[4] L. Bolduc, "GIC observations and studies in the Hydro-Québec power system," *Journal of Atmospheric and Solar-Terrestrial Physics*, vol. 64, no. 16, pp. 1793-1802, 2002-11-01 2002, doi: 10.1016/s1364-6826(02)00128-1.

[5] R. Sun, M. Mcvey, M. Lamb, and R. M. Gardner, "Mitigating Geomagnetic Disturbances: A summary of Dominion Virginia Power?s efforts.," *IEEE Electrification Magazine*, vol. 3, no. 4, pp. 34-45, 2015-12-01 2015, doi: 10.1109/mele.2015.2480636.

[6] J. S. Beland, Kevin, "Space weather effects on power transmission systems: The cases of Hydro-Québec and Transpower New Zealand Ltd.," in *Effects of space weather on technological infrastructure*, I. A. Daglis Ed., (NATO Science Series II: Mathematics, Physics and Chemistry. Netherlands: Kluwer Academic Publishers, 2004, ch. 15, pp. 287-299.

[7] M. Wik, R. Pirjola, H. Lundstedt, A. Viljanen, P. Wintoft, and A. Pulkkinen, "Space weather events in July 1982 and October 2003 and the effects of geomagnetically induced currents on Swedish technical systems," *Annales Geophysicae*, vol. 27, no. 4, pp. 1775-1787, 2009-04-14 2009, doi: 10.5194/angeo-27-1775-2009.

[8] E. E. Bernabeu, "Modeling Geomagnetically Induced Currents in Dominion Virginia Power Using Extreme 100-Year Geoelectric Field Scenarios—Part 1," *IEEE Transactions on Power Delivery*, vol. 28, no. 1, pp. 516-523, 2013-01-01 2013, doi: 10.1109/tpwrd.2012.2224141.

[9] A. Pulkkinen, E. Bernabeu, J. Eichner, C. Beggan, and A. W. P. Thomson, "Generation of 100-year geomagnetically induced current scenarios," *Space Weather*, vol. 10, no. 4, pp. n/a-n/a, 2012-04-01 2012, doi: 10.1029/2011sw000750.

[10] NERC (2014). *Reliability Standards for Geomagnetic Disturbance Operations*.

[11] Z. M. K. Abda, N. F. A. Aziz, M. Z. A. A. Kadir, and Z. A. Rhazali, "A Review of Geomagnetically Induced Current Effects on Electrical Power System: Principles and Theory," *IEEE Access*, vol. 8, pp. 200237-200258, 2020-01-01 2020, doi: 10.1109/access.2020.3034347.

[12] L. Marti, J. Berge, and R. K. Varma, "Determination of Geomagnetically Induced Current Flow in a Transformer From Reactive Power Absorption," *IEEE Transactions on Power Delivery*, vol. 28, no. 3, pp. 1280-1288, 2013-07-01 2013, doi: 10.1109/tpwrd.2012.2219885.

[13] X. Dong, Y. Liu, and J. G. Kappenman, "Comparative analysis of exciting current harmonics and reactive power consumption from GIC saturated transformers," in *2001 IEEE Power Engineering Society Winter Meeting. Conference Proceedings (Cat. No.01CH37194)*: IEEE, doi: 10.1109/pesw.2001.917055.

[14] K. Shetye and T. Overbye, "Modeling and Analysis of GMD Effects on Power Systems: An overview of the impact on large-scale power systems.," *IEEE Electrification Magazine*, vol. 3, no. 4, pp. 13-21, 2015-12-01 2015, doi: 10.1109/mele.2015.2480356.

[15] L. Bolduc, A. Gaudreau, and A. Dutil, "Saturation time of transformers under dc excitation," *Electric Power Systems Research*, vol. 56, no. 2, pp. 95-102, 2000-11-01 2000, doi: 10.1016/s0378-7796(00)00087-0.

[16] A. Haddadi, R. Hassani, J. Mahseredjian, L. Gerin-Lajoie, and A. Rezaei-Zare, "Evaluation of Simulation Methods for Analysis of Geomagnetic Disturbance System Impacts," *IEEE Transactions on Power Delivery*, vol. 36, no. 3, pp. 1509-1516, 2021-06-01 2021, doi: 10.1109/tpwrd.2020.3010195.

[17] P. K. Base, *Applications of PSCAD/EMTDC*, 2008. [Online]. Available: https://www.pscad.com/knowledge-base/download/application_20guide_202008_1.pdf.

[18] P. K. Base. "Transformer Saturation Curve Matching in PSCAD™/EMTDC™." https://www.pscad.com/knowledge-base/article/561 (accessed July 13, 2021).
[19] P. R. Price, "Geomagnetically induced current effects on transformers," *IEEE Transactions on Power Delivery*, vol. 17, no. 4, pp. 1002-1008, 2002-10-01 2002, doi: 10.1109/tpwrd.2002.803710.